Available online at www.sciencedirect.com
SCIENCE DIRECT
Applied Surface Science 252 (2006) 3984–3988
applied surface science
www.elsevier.com/locate/apsusc

Quantitative measurement of image intensity in transmission electron microscope images

Wenbang Qu [a,*], Chris Boothroyd [b], Alfred Huan [b]

[a] Department of Physics, 2 Science Drive 3, NUS, Singapore 117542, Singapore
[b] Institute of Materials Research and Engineering, 3 Research Link, Singapore 117602, Singapore

Available online 20 October 2005

Abstract

We have made a thorough comparison of the ability of image simulations to predict the contrast in high-resolution electron microscope lattice images of GaAs. Simulations of the diffracted beam intensities from thickness fringes generally agreed with observations to within ~20% over a range of GaAs thicknesses up to 150 nm. Likewise, simulations of lattice images agreed qualitatively with experimental lattice images over a range of defocus and sample thicknesses up to 20 nm. However, using the same parameters as for the diffracted beam intensities, lattice fringe amplitudes were calculated to be typically two to three times higher than observed experimentally.

PACS: 68.14.Nm

Keywords: High-resolution transmission electron microscopy; Lattice images; Energy-filtered images; Stobbs factor

1. Introduction

With quantitative high-resolution electron microscopy, it should be possible to determine atom positions and types by comparison of focal series of images with simulations. However, most investigations have found that the contrast in experimental images is usually much less than is predicted by simulations, typically by a factor of around three [1–3]. This problem is under active investigation and possible causes of this discrepancy have been discussed [4]. Investigations have shown that diffracted beam intensities, as measured either on convergent beam patterns or thickness fringes, can be predicted well at high thickness [5]. This suggests that the discrepancy lies either in the calculation of diffracted beam intensities at low thickness, or in the high-resolution imaging part of the calculation of lattice images where the effects of the objective lens are included [6–8].

In this paper, we aim to narrow down the possible errors in simulations by measuring both thickness fringe profiles and lattice fringe intensities from the same material, a 90° cleaved wedge sample of GaAs. Our aim is firstly to determine as many as possible of the simulation parameters independently of the experimental images, then match the remaining parameters to experimental thickness fringe profiles from a range of diffracted beams. This provides us with a set of simulations, which we can be sure reproduce the diffracted beam intensities as a function of thickness well. We then use these parameters to simulate lattice images for comparison with experimental lattice fringe amplitudes.

2. Experimental

In this experiment two Philips CM300 FEG electron microscopes operated at 297 kV was used to record thickness fringes and lattice images from GaAs 90° cleaved wedge specimens in the ⟨0 0 1⟩ orientation. Images were energy filtered using Gatan imaging filters with a slit width of 10 eV, which is narrow enough to exclude all plasmon scattering, but will not exclude phonon scattering. The 90° angle of this specimen means that the crystal thickness can be easily determined as twice the distance from the edge of the specimen and the cleaving process minimises contamination and surface damage.

Bright-field and dark-field images of thickness fringes were taken for all four 2 0 0, 2 2 0 and 4 0 0 reflections using an

* Corresponding author. Fax: +65 6777 6126.
E-mail address: g0301192@nus.edu.sg (W. Qu).

0169-4332/$ – see front matter © 2005 Elsevier B.V. All rights reserved.
doi:10.1016/j.apsusc.2005.09.031

objective aperture of radius 5.0 mrad. The dark-field images were taken by displacing the objective aperture to the respective beam rather than tilting the incident illumination. While such non-centred dark-field images suffer a slight loss of resolution with respect to centred dark-field images, this method does ensure that the orientation of the incident beam with respect to the crystal is exactly the same for all images. Thickness fringe profiles were simulated using the EMS [9] Bloch wave program bz2.

A focal series of 10 energy-filtered high-resolution images was taken at the ⟨0 0 1⟩ zone axis with an objective aperture of radius 17.6 mrad (8.9 nm^{-1} radius, includes 4 2 0 but excludes 4 4 0) used to provide a known maximum scattering angle. The defocus and astigmatism of each image was determined from the amorphous surface layer by the phase correlation and focal series reconstruction method of Meyer et al. [10]. Images were simulated using the EMS [9] multislice program ms1 for thickness steps of 0.565 nm assuming parallel surfaces and image processing carried out using Semper [11], with both programs running on a Silicon Graphics workstation. 2 0 0, 2 2 0 and 4 0 0 lattice fringe amplitudes were determined from Fourier transforms of 2×2 unit cell areas cut from the experimental and simulated images [12].

3. Thickness fringes

Sections of the experimental bright-field and dark-field thickness fringes were projected over a distance of 150 nm parallel to the edge of the crystal using Semper and are shown as solid lines in Fig. 1. All intensities were normalised so that the incident intensity is 1. The thickness fringes from each set of symmetry related reflections were not the same, suggesting a small degree of crystal tilt.

For simulating the thickness fringes we need to determine the Debye–Waller factor, absorption and crystal tilt that best match all the thickness fringe images. The Debye–Waller factor determines the spacing of the thickness fringes, the absorption changes the rate at which the intensity decays with thickness as well as affecting the thickness fringe spacing, while the crystal tilt affects the fringe spacing and the asymmetry between opposite pairs of reflections. Finding a consistent set of values requires trial and error starting from values reported elsewhere. Debye–Waller factors typically used for GaAs are 0.0062 nm^2 for Ga and 0.0049 nm^2 for As [13,14], 0.0066 nm^2 for both [15,16] and 0.01 nm^2 for both [7]. Our value of 0.01 nm^2, found by fitting our thickness fringes, is the same as that found by Dunin-Borkowski et al. [7] for a similar thickness fringe experiment and is significantly larger than the values determined by other methods. That this value is larger than expected suggests the possibility of beam damage as found by Dunin-Borkowski et al. [7]. Reported values for absorption (V'_g/V_g) range from 0.05 [17,18] to 0.07 [7] with our value being 0.077. Absorption models the loss of electrons from the elastically scattered beams by all mechanisms, with phonon scattering and plasmon scattering being the most significant. The amount of phonon scattering present in the images will depend on the objective aperture size used and this will explain some of the variation between reported values. The crystal tilt that best fitted the asymmetry between the beams was 0.44 mrad.

The experimental and simulated thickness fringe intensities agree over most of the thickness range to within about 20%. The most significant discrepancies are at the first thickness fringe (dark in bright-field and bright in dark-field) for the 0 0 0 and 2 2 0 reflections and to a lesser extent at other maxima and minima. This is significant because it is at a thickness used for

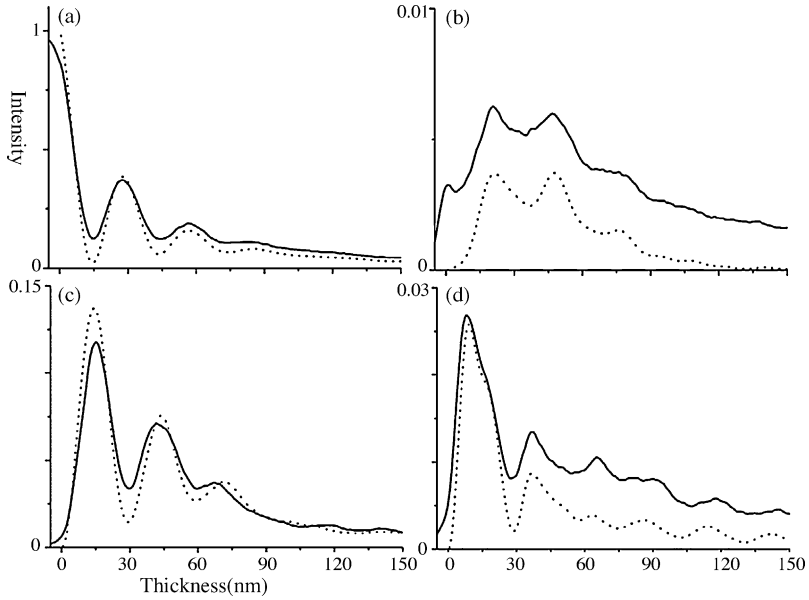

Fig. 1. Thickness fringe intensities as a function of sample thickness for (a) 0 0 0, (b) 2 0 0, (c) 2 2 0 and (d) 4 0 0 beams for a 90° wedge shaped GaAs crystal at [0 0 1]. Experimental measurements are shown as solid lines and simulations as dotted lines. An example of one of the four equivalent reflections for (b)–(d) is shown; the other three profiles differed owing to the presence of a small amount of crystal tilt.

lattice imaging and is consistent with previous findings [7]. Even so, the greatest discrepancy is about a 15% overestimate for the 2 2 0 beam at 15 nm. The average level of the 2 0 0 and to a lesser extent the 4 0 0 beams is experimentally higher than the simulations, most likely due to the contribution from the thin amorphous surface layer. In addition, there is a small peak in the 2 0 0 intensity near the specimen edge that probably also comes from the amorphous layer. At its maximum, the 2 0 0 beam intensity is only about 0.006 (cf. the 2 2 0 beam, 0.12), so that its contribution to a lattice image will be small.

4. Lattice images

For simulating lattice images there are many more parameters that need to be determined than for diffracted beam intensities. As far as possible these were determined independently of the images being simulated. The focal spread (5 nm) was determined from the energy width of the zero loss peak in an energy loss spectrum. The beam divergence (0.6 mrad) was a typical value determined from other sets of images taken under the same conditions. Although this is rather large for a field-emission gun microscope, beam divergence has only a small effect on images close to focus. The Debye–Waller factor used (0.01 nm^2 for both Ga and As) was determined from the best fit to the thickness fringe intensities. Beam tilt was assumed to be zero because the microscope was aligned to the coma-free axis before the lattice images were taken.

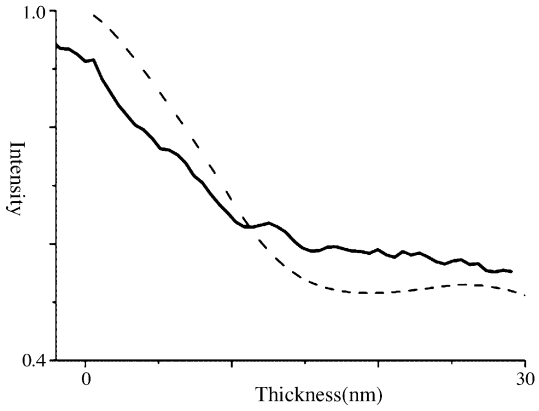

Fig. 2. Mean intensity of the GaAs lattice fringe image at defocus −40 nm. Solid line, experimental image; dotted line, simulation.

Some parameters could not be determined independently and had to be determined from the experimental images. Phonon scattering occurs between the beams in the diffraction pattern. Thus absorption will be lower than the value determined for the thickness fringes (0.077) because with a larger objective aperture (17.6 mrad) more phonon scattering is included. As a result, the absorption value used (0.055) was determined to match a plot of the mean intensity of the lattice images versus thickness (Fig. 2). The lattice images were taken in a different session and on a different microscope to the thickness fringe images, so the crystal tilt needed to be re-

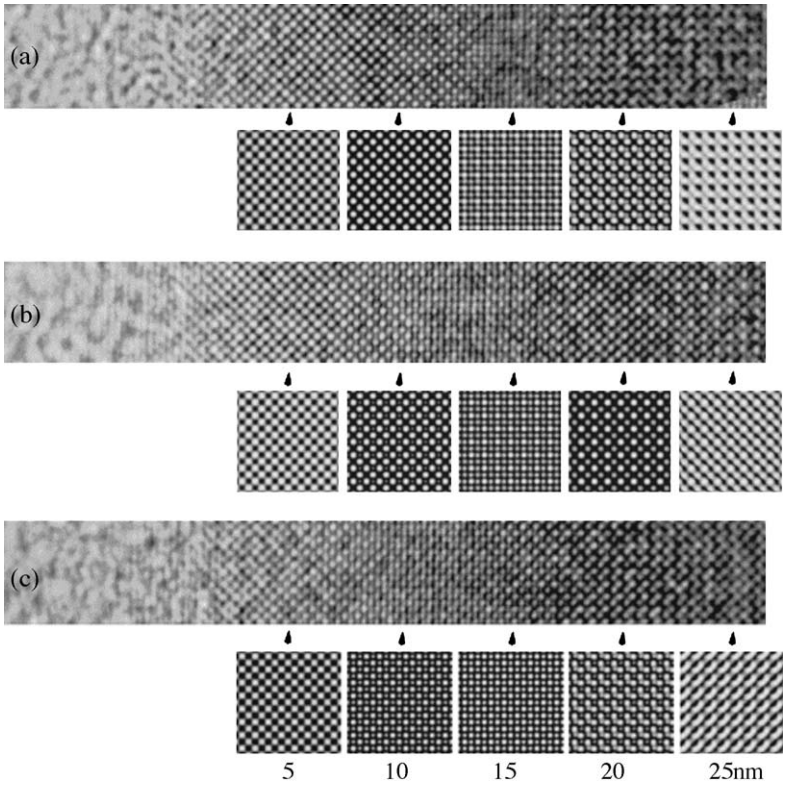

Fig. 3. Experimental and simulated lattice images from the edge of a GaAs crystal identical to that used for Fig. 1 and taken with defoci (a) −40 nm, (b) −64 nm and (c) −89 nm.

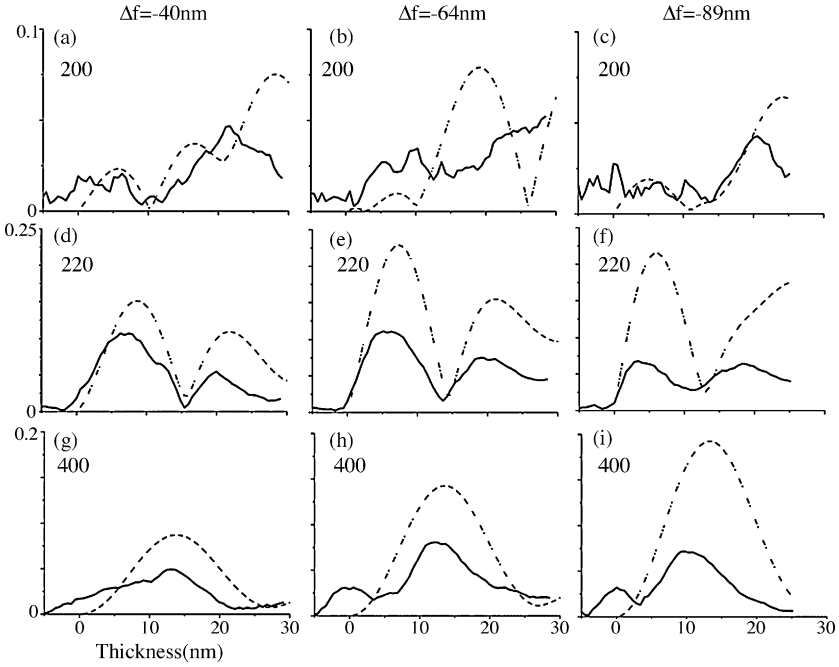

Fig. 4. 2 0 0, 2 2 0 and 4 0 0 lattice fringe amplitudes measured from the three experimental (solid line) and simulated (dotted line) images in Fig. 3. An example of only one of the two perpendicular lattice fringes is shown for each beam.

determined. It was found by trial and error based on a comparison of the pattern of the lattice images and the plots of lattice fringe amplitude versus thickness (particularly the minima in these plots) with simulations at all defocus values. Vibration is generally the most difficult parameter to determine independently. It covers any effect that removes high-frequency information from the final images such as sample vibration and imperfections in the imaging system. Its effect on diffractograms of amorphous material is very similar to that of focal spread and is often masked by beam convergence. Our approach was to assume all aspects of vibration, including the point-spread function of the detector, could be modelled as a gaussian damping of the high frequencies in the image. Thus, vibration will affect the amplitude of the 4 0 0 fringes much more than that of the 2 2 0 or 2 0 0 fringes. We thus chose a value of vibration (0.02 nm) that gave a similar ratio of simulated to experimental fringe amplitudes for the 2 0 0, 2 2 0 and 4 0 0 fringes for all defoci. By doing this we are in effect using the vibration to reduce the simulated 4 0 0 fringe amplitudes to a value nearer to the experimental 4 0 0 fringe amplitudes and making the assumption that this is valid.

Lattice images and selected simulations for three of the defoci (with the change of exit surface defocus with thickness allowed for) are shown in Fig. 3. It can be seen that qualitatively the pattern of the simulations matches the experimental images over the full range of thickness and defocus rather well. For most defoci the 2 2 0 fringes are strong near the specimen edge and the 4 0 0 fringes strong at about 15 nm thickness where the 0 0 0 beam is at a minimum. The effects of crystal tilt become more obvious in the thicker regions and are reflected in the simulations (e.g. −40 nm defocus at 20 nm thick and −89 nm defocus and 20 nm thick).

2 0 0, 2 2 0 and 4 0 0 lattice fringe amplitudes as a function of thickness for both the experimental and simulated lattice images are shown in Fig. 4. The positions of the minima in all three-lattice fringes agree well with the experimental lattice fringe amplitudes, although the experimental minima are less well defined. Likewise the relative amplitudes of the 2 2 0 and 4 0 0 fringes agree well. The experimental 2 0 0 fringe amplitudes show very poorly defined minima and appear as a gradual rise in amplitude in contrast to the oscillations in the simulated 2 0 0 fringe amplitude.

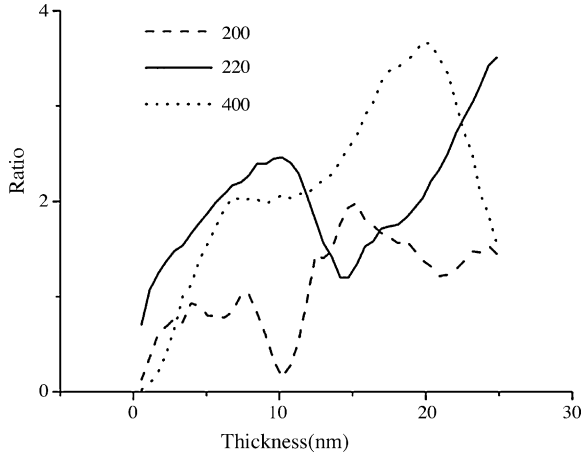

Fig. 5. Ratio of mean simulated lattice fringe amplitude to mean experimental lattice fringe amplitude of the three defoci shown in Fig. 4. This ratio (the Stobbs factor), which for a perfect match would be 1 at all thicknesses, represents the amount by which image simulations overestimate the experimental fringe amplitude.

However, the most significant discrepancy is in the overall fringe amplitudes, which are about two times greater in the simulations than in the experimental images. This can be seen more clearly in Fig. 5, which plots the ''Stobbs factor'', the ratio of the simulated to experimental fringe amplitudes as a function of sample thickness averaged over all defoci. We see that the Stobbs factor is similar for the 2 0 0, 2 2 0 and 4 0 0 lattice fringes. This is a consequence of the method used to determine vibration and is consistent with the observation that the Stobbs factor is the same for different spatial frequencies as found by Boothroyd for amorphous carbon [19].

We also see that the Stobbs factor increases with specimen thickness from a value of around 1 at 5 nm to between 2 and 4 at 25 nm. This strongly suggests that surface effects, such as the obvious amorphous layer or surface reconstructions, are not the cause of the Stobbs factor as these would be expected to have a smaller contribution at high thicknesses.

5. Conclusion

Once again, we find that after careful comparison, simulated lattice fringe amplitudes are larger than experimental lattice fringe amplitudes. This is so even though all of the beams contributing to the image intensity were measured via thickness fringes and found to be predicted correctly to within about 10%. We must conclude that the error lies in the calculation of the effects of the objective lens or the addition of stray scattering, not in the calculation of the beam intensities. We also find that the ratio of the simulated to experimental lattice fringe amplitude increases with sample thickness. This suggests that surface effects are not responsible for the discrepancy.

Acknowledgements

We are grateful to Dr. Rafal Dunin-Borkowski, Dr. Paul Midgley and the Department of Materials Science and Metallurgy, University of Cambridge, for the use of their electron microscope and for many useful discussions.

References

[1] M.J. Hytch, W.M. Stobbs, Ultramicroscopy 53 (1994) 191.
[2] C.B. Boothroyd, R.E. Dunin-Borkowski, W.M. Stobbs, C.J. Humphreys, in: D.C. Jacobson, D.E. Luzzi, T.F. Heinz, M. Iwaki (Eds.), Proceedings of the MRS Symposium, vol. 354, Pittsburgh, 1995), p. 495.
[3] K.V. Hochmeister, F. Phillipp, in: C.O.E.S.O. Microscopy (Ed.), Electron Microscopy 96, vol. 1, Brussels, 1998, p. 418.
[4] C.B. Boothroyd, J. Microscopy 190 (1998) 99.
[5] D.M. Bird, M. Saunders, Ultramicroscopy 45 (1992) 241.
[6] J.M. Zuo, J.C.H. Spence, M. O'Keeffe, Phys. Rev. Lett. 61 (1988) 353.
[7] R.E. Dunin-Borkowski, R.E. Schaublin, T. Walther, C.B. Boothroyd, A.R. Preston, W.M. Stobbs, in: D. Cherns (Ed.), Proceedings of the Electron Microscopy and Analysis Group Conference on EMAG, vol. 147, IOPP, Bristol, 1995, p. 179.
[8] J.C.H. Spence, Mater. Sci. Eng. R 26 (1999) 1.
[9] P.A. Stadelmann, Ultramicroscopy 21 (1987) 131.
[10] R.R. Meyer, A.I. Kirkland, W.O. Saxton, Ultramicroscopy 92 (2002) 89.
[11] W.O. Saxton, T.J. Pitt, M. Horner, Ultramicroscopy 4 (1979) 343.
[12] C.B. Boothroyd, R.E. Dunin-Borkowski, Ultramicroscopy 98 (2004) 115.
[13] R. Saravanan, S.K. Mohanlal, K.S. Chandrasekaran, Acta Cryst. A 48 (1992) 4.
[14] C.B. Boothroyd, J. Electron Microcopy 51 (supplement) (2002) S279.
[15] T. Matsushita, J. Hayashi, Phys. Status. Solid. 41 (1977) 139.
[16] J.S. Reid, Acta Cryst. A 39 (1983) 1.
[17] C.R. Hall, P.B. Hirsch, G.R. Booker, Phil. Magn. 14 (1966) 979.
[18] S. Thoma, H. Cerva, Ultramicroscopy 35 (1991) 77.
[19] C.B. Boothroyd, Ultramicroscopy 83 (2000) 159.